2015-01-1167
Published 04/14/2015

doi:10.4271/2015-01-1167
saealtpow.saejournals.org

Experimental Test Campaign on a Battery Electric Vehicle: Laboratory Test Results (Part 1)

Michele De Gennaro, Elena Paffumi, Giorgio Martini, and Urbano Manfredi
EC Joint Research Centre

Stefano Vianelli
EURINS srl

Fernando Ortenzi and Antonino Genovese
ENEA

ABSTRACT

The experimental measurement of the energy consumption and efficiency of Battery Electric Vehicles (BEVs) are key topics to determine their usability and performance in real-world conditions. This paper aims to present the results of a test campaign carried out on a BEV, representative of the most common technology available today on the market. The vehicle is a 5-seat car, equipped with an 80 kW synchronous electric motor powered by a 24 kWh Li-Ion battery. The description and discussion of the experimental results is split into 2 parts: Part 1 focuses on laboratory tests, whereas Part 2 focuses on the on-road tests.

As far as the laboratory tests are concerned, the vehicle has been tested over three different driving cycles (i.e. NEDC, WLTC and WMTC) at two different ambient temperatures (namely +25 °C and −7 °C), with and without the use of the cabin heating, ventilation and air-conditioning system. To further investigate this aspect, the European draft MAC test procedure has been also applied. The results show that the energy consumption of the vehicle ranges from 157 to 278 Wh/km (i.e. equivalent gasoline consumption from 1.8 to 3.1 l/100km) and the grid-to-wheel efficiency approximately ranges from 46.6% to 79.0%, depending on the test conditions. The driving range measured with the full-length test procedure results to be between 112 and 127 km, whereas the one-cycle abbreviated range test approach provides values between 74 and 131 km. The multi-cycle procedure has been also applied, in order to investigate the sensibility of the calculated range to different numbers of cycles considered.

The paper provides the reader with a detailed description of the measurement equipment and setup adopted during the tests, setting the background for future technical analyses and experimental campaigns.

CITATION: De Gennaro, M., Paffumi, E., Martini, G., Manfredi, U. et al., "Experimental Test Campaign on a Battery Electric Vehicle: Laboratory Test Results (Part 1)," *SAE Int. J. Alt. Power.* 4(1):2015, doi:10.4271/2015-01-1167.

INTRODUCTION

Determining the energy consumption and efficiency of Battery Electric Vehicles (BEVs) under different driving conditions is a key topic to understand the potential benefits of this technology in replacing conventional fuel vehicles. Although the conventional fuel vehicles have substantially increased their efficiency over the last decade [1], in order to reduce the dependency on oil and as well as pollutants and Greenhouse Gases (GHGs) emissions [2, 3], new low-carbon vehicles technologies (i.e. Hybrid Electric Vehicles, (HEVs), and BEVs) are constantly expanding their market shares.

HEVs technology basically aims to complement the combustion engine technology by means of energy recuperation and boosting and/or an alternative propulsion system based on an electric motor. In particular, the energy recuperation system recovers part of the kinetic energy which the vehicle dissipates during braking and deceleration driving phases. This energy is typically stored in a battery and then used to boost the vehicle during the accelerations and/or provide a short full-electric driving range to the vehicle. HEVs are typically equipped with a small sized battery and a small-to-medium sized electric motor, designed to support and/or replace combustion engine torque, especially at low rotational speeds, where the combustion engine is characterized by low fuel efficiency. Such technology can

be arranged in many different configurations (i.e. micro, mild and full hybrid) according to the battery capacity and costs, the drivetrain architecture (i.e. serial/parallel/through-the-road hybrids) and the relative power of the electric motor with respect to the total power installed (i.e. Degree of Hybridization, DoH). Although HEVs technology enables to increase the overall efficiency of the vehicle, constituting a valuable technological step forward with respect to conventional fuel vehicles, this increase is not always linked to a decrease of gaseous emissions, as shown by the authors [4].

On the other hand BEVs constitute a paradigm shift compared to conventional fuel vehicles, although their popularity is still limited by their high purchase cost (mainly due to the cost of the battery) and the doubts of the consumers on their effective driving range and usability. Beyond these limitations, previous studies from the authors suggest that the relatively short range of the current generation of BEVs is not a strict limitation, and approximately one-fourth of the urban cars could be shifted from conventional fuel vehicles to BEVs [5] without any negative impact due to the shorter range. This share increases to approximately half of the fleet by accepting a very limited modal-shift [6]. These studies are based on a large-scale activity datasets acquired on conventional fuel vehicles from private citizens, and highlight that the actual potential of BEVs might go far beyond the common expectations. However they rely on the fine-tuning of the numerical models and, therefore, on an accurate experimental estimate of BEVs' energy consumption in real driving conditions.

The objective of this study is to provide the scientific community with the results of a test campaign carried out on a BEV. This vehicle is representative of the most common BEVs technology available on the market today. The tests have been carried out in the laboratories of the Joint Research Centre of the European Commission (JRC), in collaboration with the Italian National Agency for new Technologies, Energy and Sustainable Economic Development (ENEA). The test campaign is carried out in the frame of the pre-normative research activities of the JRC in support of the development of the type approval regulation, and consists of two parts: Laboratory Tests (i.e. Part 1) and On-road Tests (i.e. Part 2).

The laboratory tests are targeted to determine the energy consumption, energy efficiency and driving range over different driving cycles (i.e. NEDC [7, 8, 9, 10], WLTC, WMTC [11] and MAC [12]) and ambient conditions. Ambient temperatures of +25 °C and −7 °C are considered, as prescribed by the current type approval test procedures for passenger cars, and the tests are carried out with and without the Heating, Ventilation and Air-Conditioning (HVAC) system in operation (in cooling and heating mode).

The on-road tests have the objective of determining the same parameters (i.e. energy consumption and range) over three different real-driving routes, ranging from 60 to 90 km each, with a driving time ranging approximately from one and half to two and half hours, [13]. The routes have been designed to include different pathways (i.e. city driving, rural driving and highway), and are partially based on the criteria established for the on-road emissions tests for conventional fuel vehicles with Portable Emissions Measurement System (PEMS), [14]. These include the full range of driving speeds which might be encountered in real-world driving, the effect of road slope and altitude variation, as well as the effect of the different driving modes (i.e. normal drive and economic driving mode (ECO) drive). The shares of the driving time during which the acceleration pedal position is above or equal to 40%, and of the share of driving distance during which the vehicle speed is above or equal 50 km/h, have been used to monitor the driving style aggressiveness, as per [15] and [16], setting the basis for future studies to define eco-driving rules and eco-indices, or correlating HEVs gaseous emissions to the driving style, [17, 18].

In order to measure the energy consumption, the vehicle has been instrumented with a data logger capable to monitor in real-time the energy flows from and to the different vehicle's sub-systems. A detailed description of this measurement system and its configuration layout is also provided.

These two parts of the test campaign allow a direct comparison of the results, in order to obtain a comprehensive overview of the energy consumption and driving range in type approval and real-driving test conditions for the tested vehicle. This will contribute to the correlation between type approval duty cycles and real-world driving cycles as well as to the evaluation of the impact of auxiliary systems on the driving energy consumption not prescribed by the current regulation.

EXPERIMENTAL SET-UP

Test Vehicle and Measurement Points

The BEV adopted for this study is a 5-seat car, with an empty weight of 1520 kg and powered with a 80 kW / 280 N·m synchronous electric motor in front-wheel driving configuration. The vehicle is equipped with a 96-cells Lithium-Ion battery, accounting for a 24 kWh nominal capacity and approximately 360 V nominal voltage. The vehicle's main characteristics are summarized in Table 1, while its schematic representation is provided in Figure 1. With reference to this figure the vehicle's main sub-systems are:

- Charger unit and AC/DC converter: it converts the 3.3/6.6 kW Alternating Current (AC) from the grid to Direct Current (DC) for the high-voltage battery. The current from the DC charging flows directly into the high-voltage battery;
- High-voltage battery: it is the main energy storage device of the vehicle;

- Inverter unit: it converts DC from the high-voltage battery to 3-phases AC for the Electric Motor (i.e. EM);
- DC/DC converter: it converts the DC from the high-voltage battery to low-voltage DC for the auxiliary systems (i.e. air-conditioning and cabin ventilation system, lights, wipers, etc.);
- Heater: a 5 kW DC resistance to heat-up the cabin, directly connected to the high-voltage battery.

Table 1. Test vehicle characteristics.

Architecture	BEV
Propulsion	Synchronous electric motor
Max. Power [kW]	80
Max. Torque [N·m]	280
Mass [kg]	1520
Battery	24 kWh – 96 Li-Ion cells 360 V (nominal voltage)

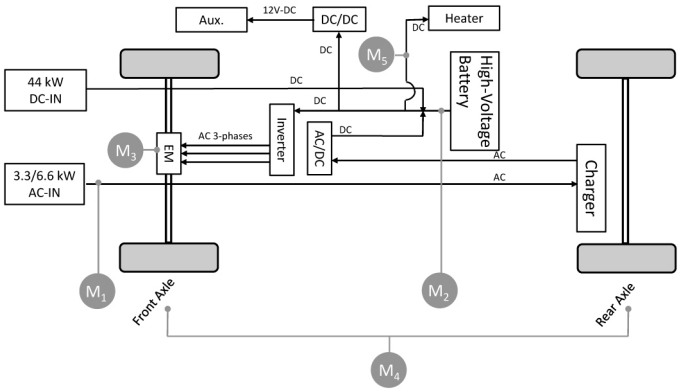

Figure 1. BEV schematic representation and measurement points (see Table 2).

Please note that the cooling system of the cabin is loaded on the low-voltage auxiliaries (i.e. downstream with respect to the DC/DC), whereas the heating system is directly loaded on the high-voltage battery.

All the sub-systems are inter-connected by several power lines. The schematic representation of Figure 1 reports the main power-line, each depicted with an arrow; single arrows refer to the mono-phase AC power lines (AC label), the low-voltage DC power lines (DC-12V label), and the high-voltage DC power lines (DC label). The three parallel arrows refer instead to the 3-phases AC power line (AC 3-phases label). The vehicle is also equipped with a 44 kW DC fast charging line. Gray circles in Figure 1 represent the measurement points on the vehicle used to monitor the energy flows, and used for the analyses reported in this article. A detailed description of these measurement points is provided in Table 2.

Table 2. Measurement points summary (see Figure 1).

Measurement point label	Description
M_1	Energy from the grid to the high-voltage battery [Wh]; (acquired directly on the recharging station)
M_2	Current [A] and Voltage [V], from the high-voltage battery feeding the inverter, the low-voltage auxiliary systems and the heating system → energy outflow from the battery to all subsystems [Wh]; (acquired both by CANbus and current clamp. Note that it can be also calculated by SOC scaling)
M_3	Rotational speed [rpm] and torque [N·m] of the electric motor → mechanical energy of the electric motor [Wh]; (acquired by CANbus)
M_4	Energy at the wheel [Wh]; (calculated by (1)).
M_5	Current [A] and Voltage [V], from the high-voltage battery to the heater → energy from the battery to the cabin heating system [Wh]; (acquired by current clamp)

Table 3. Parameters to calculate the energy consumption at the wheel (i.e. measurement point M4), according to (1).

Parameters	Description	Value
m_v	Vehicle mass: - Laboratory tests: = curb weight + driver (75 kg). - On-road tests: = curb weight + driver (75 kg) + one passenger (70 kg) + equipment (5 kg).	1595 [kg] 1670 [kg]
g	Gravity acceleration.	9.81 [m/sec^2]
μ	Road friction coefficient.	0.0127 (non-dim.)
ρ	Air density.	1.18 [kg/m^3]
c_x	Vehicle drag coefficient.	0.28 (non-dim.)
A	Vehicle front surface area.	2.27 [m^2]
α	Road slope angle.	Variable, [rad]
v_{wind}	Wind speed velocity	[m/sec]
$sign$	Sign function, it determines the sign of the algebraic sum $(v + v_{wind})$	(non-dim).

The measurement at the stage M_1 is acquired directly on the 3.3/6.6 kW AC recharging station, by monitoring the electric energy required to recharge the battery. The measurement at the stage M_2 is acquired in double mode, i.e. via the vehicle CANbus and via a current clamp directly mounted on the battery output power-line. Additionally the energy outflow from the battery (i.e. M_2) can be also calculated by considering the SOC variation, scaled on the nominal capacity of the battery. The measurement at the stage M_3 is acquired only via CANbus, whereas the measurement at the stage M_5 is acquired only via current clamp. The energy at the wheel (i.e. stage M_4) is calculated by (1), according to the parameters reported in Table 3.

$$E_{wheel} = \int_{t_{in}}^{t_{fin}} m_V a\ t\ + m_V \cdot g \cdot sin\ \alpha\ t\ + \mu \cdot m_V \cdot g \cdot cos\ \alpha\ t\ + sign(v(t) + v_{wind}(t)) \frac{\rho}{2} c_x A (v(t) + v_{wind}(t))^2 \cdot v(t) dt \quad (1)$$

These parameters have been kept constant, regardless the change of the environmental conditions, such as ambient temperature, humidity and atmospheric pressure (e.g. variations due to the altitude during the on-road tests).

Please note that application of the formula (1) is particularly difficult for on-road tests, because of the inaccuracies in the real time measurement of the road slope angle α, the wind speed and the wind direction during the test. In particular the road slope angle has been derived from the altitude maps of the on-road routes, given the vehicle instantaneous position by GPS records, according to [19]. These values have been also integrated with GPS altitude measurements appropriately smoothed and processed, and a sensitivity technique analysis has been carried out to assess the effect of this smoothing on the derived road slope angle. The wind speed and direction during the on-road driving have been instead measured by an ultrasonic sensor (see *Measurement Equipment* section) and the recorded values have been submitted to a smoothing process too. Also the of the road friction coefficient was particularly difficult to quantify for the on-road tests, due to the changes in the road surface (i.e. inhomogeneous asphalt) and tire dynamic. Equations from the literature related to the wheel dynamic have been applied to perform a sensitivity study of these effects; however this represents only a simplified attempt to address these issues and dedicated future study are needed to improve the results to derive on-road efficiency.

The tested vehicle is three years old (i.e. registered in 2011 and tested in 2014), with a total mileage of approximately 5,000 kilometres. Therefore it is likely that its battery performance is slightly degraded by aging compared to a brand new vehicle. For example we noticed during our tests that the State-of-Charge (SOC) indicator at a CANbus level did not allow recharging above a variable threshold between 86% and 90% (upper bound) and discharging below 3% (lower bound). This has been also confirmed by battery energy-in measurements in M_2 (i.e. via vehicle CANbus) during overnight full recharge tests, which allowed an average value of recharge energy equal to 20.5 kWh (i.e. 85% of the nominal energy capacity). For this reason we have decided to use this value to scale the driving range test results, later referred as battery usable SOC.

Measurement Equipment

The measurement equipment installed on the vehicle consists of a data logger based on a modular chassis with 8 configurable slots (Figure 2, from label 4 to 11). Its operative temperature ranges from −40 to +70 °C, it is dust-proof and shock resistant, designed to be powered with 9-30 volts DC (i.e. Power-in label 1 in Figure 2) to be mounted on-board of the tested vehicle. It embeds a dual-core CPU plus a configurable FPGA chip. The data can be either stored on the embedded 1 GB non-volatile flash memory (expandable via USB-port) or downloaded via the Ethernet port (i.e. Output-port, label 2 in Figure 2). This port can be also used to configure the modules for live telemetry.

The structure of the data logger is:

- GPS, label 3 in Figure 2: serial port for GPS-receiver, it works with NMEA standard sentences, providing the system with: dynamic update of absolute UTM timestamp, absolute geographical position, vehicle speed related to ground, vehicle course related to North, signal quality and number of satellites.
- Power (V-in), labels 4 and 6 in Figure 2: two groups of 3 channels each with voltage input for single or three-phases power measurements. Voltage input up to 300 V rms, 24 bits, differential, simultaneous sampling, integrated anti-alias filters, 50 k-samples/second per channel, (i.e. bandwidth at 24.6 kHz).
- Power (I-in), labels 5 and 7 in Figure 2: two groups of 4 channels each with current input for single or three-phases power measurements. Current input up to 1600 A rms (with 1600:5 transformer), 24 bits, differential, simultaneous sampling, integrated anti-alias filters, 50 k-samples/second per channel, (i.e. bandwidth at 24.6 kHz).
- Analog-in, label 8 in Figure 2: 16 channels for analogic inputs at the voltage of ±10 V, 16 bits, differential, 250 k-samples/second multiplexed.
- Thermocouples, label 9 in Figure 2: 16 channels, 24 bits, integrated with a Cold Junction Compensation (CJC), supporting thermocouples of types J, K, T, E, N, B, R, S.
- Frequency-in, label 10 in Figure 2: 8 channels for frequency-dependent digital acquisition plus 32 channels for logical states. Switching speed at 7 µ-seconds, inputs voltage up to 24 V.

CANbus-in label 11 in Figure 2: 2 independent CAN High Speed ports at 11 bits and 29 bits messages IDs, baud rate up to 1 Mbps, interfaced with the Electronic Control Unit (ECU) for both standard (i.e. DBC, OBD, FMS) and non-standard (i.e. editable) protocols.

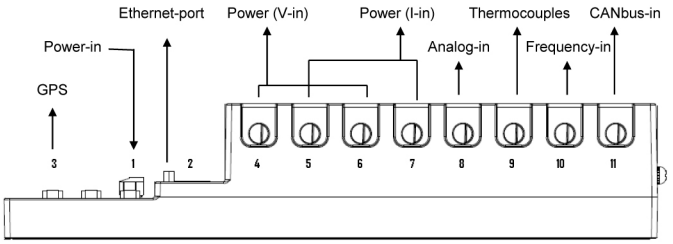

Figure 2. Schematic representation of the measurement system.

The data logger modules are based on standard components from [20] and assembled with a customized software interface from [21]. This interface is capable to perform live-data visualization, data synchronisation and remote storage as well as control the configuration of the system. The system has been configured for the present test campaign according to the measurement points described in Table 2.

The modules 4 to 7have been used for the inverter acquisition, (i.e. 3-phases voltages and currents acquired by means of current transformer); the module 6 for the recording of the AC recharging pilot signal [22, 23]; the module 8 has been used for DC acquisition, (i.e. from and to the high-voltage battery and heater system acquired by means of current clamps based on Hall effect) plus ambient data acquisition from a sensors array mounted on the vehicle's roof. This array implements ambient temperature, pressure and relative humidity sensors, plus wind speed and wind direction ultrasonic sensors. Module 9 has been used for cabin thermal acquisition, according to the specifications described in the European MAC draft test procedure [12], while module 11 has been used for CANbus acquisition, integrated with a GPS antenna mounted on port 3. Please note that 3-phases voltages and currents measured at the inverter have not been used for deriving the results presented in this work. Moreover GPS and ambient conditions are not relevant for laboratory tests, and therefore not reported in Part-1.

Test Facility

The tests presented in this study are performed in the **V**ehicle **E**mission **La**boratories (**VELA**) of the Joint Research Centre of the European Commission in Ispra (Italy). The laboratory tests have been carried out in the VELA-2 facility, equipped with a 4×4 chassis dynamometer (double roller bench). This facility is designed to test passenger cars and light duty trucks at different ambient temperatures ranging from −10 °C to +30 °C, and humidity of 50 ± 5%. VELA-2 is equipped also with an emission measurement system and with a driver aid system, to ensure consistent performance across all tests. A more detailed description of the facility can be found in [24].

Driving Cycles

Four test cycles have been adopted in this study and their phases are shown in Figure 3. The New European Driving Cycle (NEDC) for passenger cars [7, 8] is the current legislative cycle prescribed to determine whether a new model of Light Duty Vehicle (LDV) meets EU environmental regulations. This test-cycle is also adopted to determine the range and the energy consumption of electric vehicles, as per [9]. The NEDC cycle is divided into two parts. The first part (i.e. phase 1, four repetitions of the ECE15 cycle [10], 780 seconds, 4.06 km) simulates urban driving conditions. The second part (phase 2, one repetition of the EUDC cycle [10], 400 seconds, 6.95 km) simulates the driving conditions in extra-urban areas. In order to simplify and harmonize at global level the test procedures and in the framework of the activities of the United Nation Economic Commission for Europe (UNECE), two harmonized test cycles have been developed: the World-wide harmonized Light-duty Test Cycle (WLTC) for LDVs [11] and the World-wide Motorcycle emission Test Cycle (WMTC) for 2-wheelers. The WLTC is broken down in four phases: low speed (589 seconds and 3.09 km), medium speed (433 seconds and 4.76 km), high speed (455 seconds and 7.16 km) and extra-high speed (323 seconds and 8.25 km). These phases are designed to represent urban traffic, mixed conditions and highway conditions respectively. Similarly, the WMTC is divided into three phases: low speed (600 seconds and 4.06 km), medium speed (600 seconds, 9.11 km) and high speed phase (600 seconds, 15.73 km). These cycles are in general more dynamic than the NEDC, better representing the real-world driving conditions.

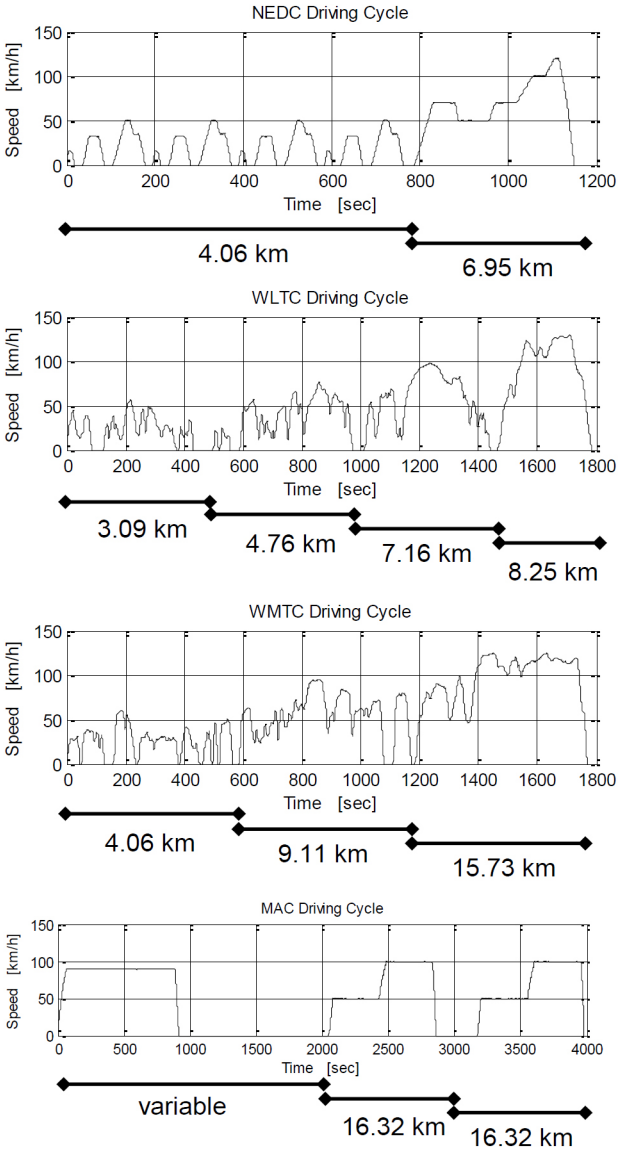

Figure 3. NEDC, WLTC, WMTC and MAC driving cycles and phases.

In order to determine the energy and fuel consumption of the HVAC system, the new Mobile Air Conditioning (MAC) cycle and test procedure is also under development [12]. This test prescribes a cycle made of three phases: the pre-conditioning phase (i.e. phase 1) plus two identical phases (i.e. phases 2 and 3), respectively with and without the HVAC system in operation. Phase 1 lasts for approximately 30 minutes at a constant speed of 90 km/h, while phases 2 and 3 last for approximately 16 minutes each, half driven at a constant speed of 50 km/h and half at 100 km/h. This test prescribes the minimum HVAC system mass flow rate (i.e. 230 kg/h), together with the monitoring of the cabin temperature in seven control points: four located on the dashboard and three behind the seats of the driver and the passenger.

The test is carried out at the ambient temperature of +25 °C, and the HVAC system of the vehicle must decrease the cabin temperature to a target value set below +15 °C. The phase 1 is designed to stabilize the cabin temperature at this temperature, while phase 2 and phase 3 are designed to compare the energy or fuel consumption of the vehicle with and without the HVAC system in operation (cooling mode). During phase 2 the HVAC system must only maintain the cabin temperature around a steady-state value.

In this study the MAC test procedure has been applied at the ambient temperatures of +30 °C and +25 °C with the HVAC system in cooling mode, as well as at −7 °C, with the HVAC system in heating mode. Although the latter test is not prescribed in the current MAC draft test, it has been performed to address the impact of the heating system on electric vehicles energy consumption at cold ambient temperature, having it a larger impact on BEVs than on conventional fuel vehicles. For all tests the HVAC system is set at the maximum power. The vehicle has been driven for 30 minutes in the phase 1 of the MAC cycle (i.e. constant speed at 90 km/h) for the +30 °C and +25 °C tests, while the phase 1 has been shortened to 15 minutes of driving plus 15 minutes of idling (keeping the HVAC system in operation) for the −7 °C test, in order to have enough energy in the battery to complete the phases 2 and 3. The energy consumption results have been reported only for these last two phases.

RESULTS

Energy Consumption Results

This paragraph describes the energy consumption results over the NEDC, WLTC, WMTC and MAC test cycles. Each test has been repeated in four different conditions, corresponding to the combination of the ambient temperatures (i.e. $T_{Amb.}$) of +25 °C and −7 °C and HVAC system (cooling mode at +25 °C, heating mode at −7 °C) switched-on and switched-off. As far as the NEDC, WLTC and WMTC driving cycles are concerned, the HVAC system has been switched-on immediately before the test (i.e. without performing the cabin temperature pre-conditioning). The MAC test cabin temperature conditioning was instead performed according to [12].

Table 4 provides the energy consumption results calculated for the driving cycles at the battery level (i.e. without considering the efficiency loss during the recharge) by the current and voltage at the battery outlet from the CANbus (i.e. M_2 according to Table 2). Each cycle is repeated twice and the results are reported for the first cycle which includes the mechanical warm-up of the drivetrain (i.e. cold-start). This effect is very small (i.e. below 2% of the combined energy consumption results reported), and it has been included to represent the worst case scenario, in terms of energy consumption.

The distance specific energy consumption in Wh/km is given per cycle phase and combined for the whole cycle, for each test condition. This consumption values have been converted to an equivalent value expressed in liters of gasoline per 100 km (i.e. liters/100km, see values in parenthesis), by applying the conversion suggested by the Environmental Protection Agency (EPA, [25]) as per (2). The energy content of the gasoline fuel has been assumed equal to 8.90 kWh/liter (i.e. 115 kbtu/gallon).

$$Consumption\ \frac{l}{100km} = Consumption\ \frac{Wh}{km} \cdot \frac{0.1123}{10} \quad (2)$$

Table 4. Energy consumption results (NEDC, WLTC and WMTC)

		NEDC [Wh/km] (l/100 km)	WLTC [Wh/km] (l/100 km)	WMTC [Wh/km] (l/100 km)
$T_{Amb.}$ = +25 ºC HVAC OFF	Phase 1	144.3 (1.62)	158.0 (1.77)	169.0 (1.90)
	Phase 2	164.1 (1.84)	173.8 (1.95)	169.1 (1.90)
	Phase 3	-	163.2 (1.83)	194.7 (2.19)
	Phase 4	-	202.5 (2.27)	-
	Combined	156.9 (1.76)	178.4 (2.00)	182.9 (2.05)
	Rec. Ratio (Battery)	7.6%	6.4%	7.2%
	Rec. Ratio (EM)	10.5%	9.8%	9.9%
$T_{Amb.}$ = +25 ºC HVAC ON	Phase 1	192.6 (2.16)	203.5 (2.28)	212.6 (2.39)
	Phase 2	175.9 (1.98)	190.1 (2.13)	182.2 (2.05)
	Phase 3	-	175.3 (1.97)	204.3 (2.29)
	Phase 4	-	209.1 (2.35)	-
	Combined	182.0 (2.04)	194.0 (2.18)	198.6 (2.23)
	Rec. Ratio (Battery)	5.6%	4.4%	5.1%
	Rec. Ratio (EM)	10.8%	8.9%	9.5%
$T_{Amb.}$ = -7 ºC HVAC OFF	Phase 1	146.9 (1.65)	198.1 (2.23)	181.4 (2.04)
	Phase 2	185.2 (2.08)	200.1 (2.25)	184.6 (2.07)
	Phase 3	-	181.4 (2.04)	214.2 (2.41)
	Phase 4	-	222.4 (2.50)	-
	Combined	171.2 (1.92)	202.0 (2.27)	200.1 (2.25)
	Rec. Ratio (Battery)	7.9%	4.7%	6.5%
	Rec. Ratio (EM)	8.9%	6.2%	8.1%
$T_{Amb.}$ = -7 ºC HVAC ON	Phase 1	240.7 (2.70)	367.1 (4.12)	305.0 (3.42)
	Phase 2	255.4 (2.87)	292.3 (3.28)	258.5 (2.90)
	Phase 3	-	250.0 (2.81)	260.9 (2.93)
	Phase 4	-	260.7 (2.93)	-
	Combined	250.0 (2.81)	278.1 (3.12)	266.6 (2.99)
	Rec. Ratio (Battery)	2.6%	1.2%	2.0%
	Rec. Ratio (EM)	8.6%	7.9%	8.1%

The energy recuperation ratio is also reported at the battery and at the EM level. At the battery level it is instead calculated by dividing the battery energy inflow by the battery energy outflow measured by CANbus current and voltage (see measurement point M_2), while, at the EM level, it is calculated by dividing the electric motor recuperated energy by the electric motor driving energy (see measurement point M_3). Both ratios are given in [%], and they provide the reader with a quick estimate of the impact of the energy recuperation on the total energy consumption for each cycle and test conditions. By comparing these ratios it can be immediately derived the behavior of the regenerative braking, highlighting which driving cycles and which test conditions allow for higher shares of

regenerated energy over the cycle. Please note that the ratio at the battery level is lower than that at the EM level, accounting for the energy losses between the battery and the EM (i.e. power lines and inverter).

The results given in Table 4 show that the energy consumption at +25 °C varies from approximately 157 to 183 Wh/km, increasing from 171 to 202 Wh/km at −7 °C, without the HVAC system. The HVAC system in cooling mode (i.e. T_{Amb} = +25 °C and HVAC ON) has an impact that can be quantified in approximately +10-15% increase of the energy consumption, while it has a higher impact in heating mode (i.e. T_{Amb} = −7 °C and HVAC ON), up to approximately +46% increase.

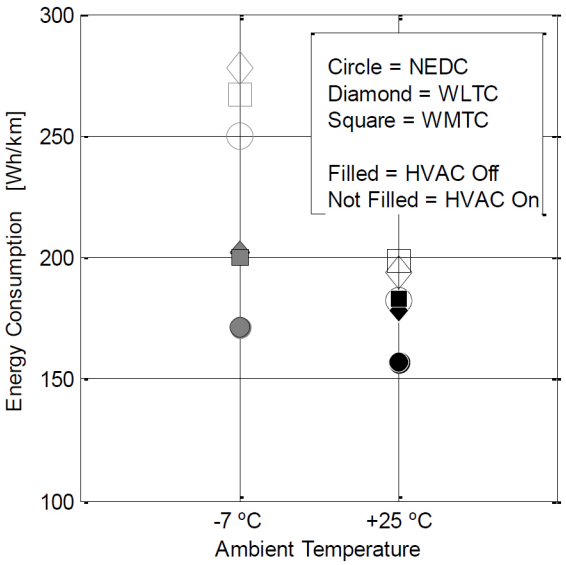

Figure 4. Energy consumption results at different ambient temperature (summary).

This is visible especially over the NEDC that, being the shorter among the considered cycles, is also the more affected by cabin temperature transient. The energy consumption results are also graphically shown in Figure 4, depending on the temperature, where it is immediately visible the effect of different ambient conditions and auxiliaries' load. Additionally the second-by-second cumulative energy consumption is given for all the tested conditions in Appendix (see Figure 6).

The recuperation ratio ranges from 7.9% to 10.8% at the EM level and from 1.2% to 7.9% at the battery level. Battery level results shows lower energy recuperation for the WLTC cycle compared to the other cycles at all temperatures. Additionally battery level recuperation at −7 °C and with the HVAC system switched-on is significantly lower compared to other test conditions. This is probably due to the fact that the regenerated energy in this condition is not stored in the battery but directly used to feed the cabin heating system. Lower recuperations are also observed for the tests at +25 °C with HVAC system switched-on in comparison to the same tests without HVAC system in operation, while the values at the EM level remain the same.

By converting the energy consumption results to the equivalent gasoline consumption, we derive a consumption ranging from 1.8 to 3.1 l/100 km (combined data), showing how BEVs are, in almost every condition, more energy efficient than conventional fuel cars, [4]. Please note that these values might increase because of the effect of the energy losses during the recharge (i.e. from the grid to the battery), not included at this stage. These will be later introduced in the *Energy Efficiency Results* section.

Table 5. Battery energy outflow measurements: sensitivity analysis

	NEDC		WLTC		WMTC	
	SOC	Clamp	SOC	Clamp	SOC	Clamp
$T_{Amb.}$ = +25 ºC HVAC OFF	-3.6%	1.0%	8.1%	3.0%	-1.2%	3.1%
$T_{Amb.}$ = +25 ºC HVAC ON	-6.6%	4.9%	0.0%	4.8%	2.1%	2.1%
$T_{Amb.}$ = -7 ºC HVAC OFF	15.5%	-18.0%	17.1%	-9.5%	5.5%	-17.5%
$T_{Amb.}$ = -7 ºC HVAC ON	28.0%	-9.6%	-0.2%	-16.5%	-6.9%	-15.5%

Table 6. Energy consumption results (MAC)

		MAC [Wh/km] (l/100 km)
$T_{Amb.}$ = +25 ºC HVAC ON	Phase 2	171.2 (1.92)
	Phase 3	159.9 (1.80)
	Ratio	+7.1%
$T_{Amb.}$ = -7 ºC HVAC ON	Phase 2	229.9 (2.58)
	Phase 3	174.2 (1.96)
	Ratio	+32.0%
$T_{Amb.}$ = +30 ºC HVAC ON	Phase 2	154.5 (1.74)
	Phase 3	148.8 (1.63)
	Ratio	+6.8%

A sensitivity analysis of the battery energy outflow measurements has also been performed. As reported above the distance-specific energy consumption values reported in Tables 4 are calculated by the current and voltage at the battery outlet from CANbus. These values might be also calculated by means of CANbus SOC scaling (referring to the nominal battery capacity of 24 kWh) and by means of DC measurement via a current clamp (Hall-effect clamps, see *Measurement equipment* section). These approaches constitute separate measurements of the energy inflow and outflow of the battery, providing an indication on the sensitivity of the accuracy of the energy consumption results. Table 5 shows the percentage deviation of the combined consumption by SOC scaling and by clamp measurement with respect to the combined energy consumption values by CANbus measurements of Table 4. This analysis shows the poor correlation of these two different measurements, especially for low ambient temperature. As far as the SOC scaling is concerned, the deviation can be explained with possible inaccuracies in the SOC calculation algorithm implemented in the vehicle CANbus, whereas as far as the DC clamp measurement is concerned, this deviation can be partially explained by a drift of the instrument (i.e. this drift has been noticed to increase over time, since the clamp zero needs a periodical reset).

Table 6 reports the distance specific energy consumption for the MAC test cycles, phases 2 and 3 for the three ambient temperatures considered, by the current and voltage at the battery outlet from CANbus (i.e. measurement point M_2). Phase 1 (i.e. variable) is not reported, being designed only to reach a steady-state cabin temperature. The recuperation ratios are also not reported, being meaningless for driving phases driven at constant speed. Instead the ratio between the energy consumption from the phases 2 and 3 is reported, to highlight the influence of the HVAC system in operation on the energy consumption.

The results show that this impact is rather limited in cooling mode (i.e. approximately +7% of increase in the energy consumption, for both +25 °C and +30 °C ambient temperatures tested), whereas a +32% increase is calculated for the HVAC system in heating mode. These results are coherent with those from the driving cycles reported in Table 4, showing a significant increase of the energy consumption with cabin heating compared to cabin cooling. The second-by-second cumulative energy consumption over the MAC driving cycle and the cabin temperatures measured during the tests are reported in appendix in Figure 7. The cabin temperature measurement points reported are: left, mid and right probe positions (corresponding to driver's head, between the driver's and the passenger's seat and behind the passenger's head) and left, mid and right duct positions (corresponding to the left, mid and right outlet of the HVAC system located on the dashboard). Note that, according to the MAC specifications, the thermocouples located on the dashboard are four: left, mid-left, mid-right and right outlet of the HVAC system. For simplicity the mid duct temperature reported here is the average between the mid-left and mid-right duct measurements. The thermocouples in the cabin show that the temperature stabilizes approximately after 10 minutes in cooling mode (reaching the MAC target value of +15 °C at the end of phase 1 for the ambient temperature equal to +25 °C), whereas it takes approximately 20/25 minutes in heating mode.

Energy Efficiency Results

The energy efficiency of the vehicle has been calculated for the NEDC, WLTC and WMTC tests according to the diagram proposed in Figure 5, based on the measurements points described in Table 2.

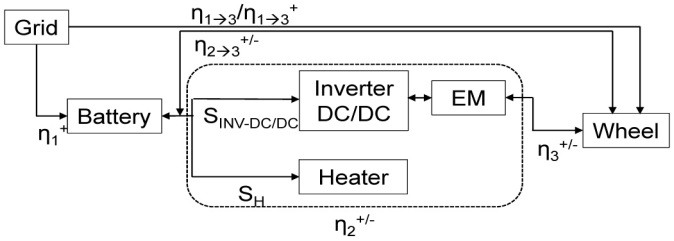

Figure 5. Efficiency cascade, from the grid to the wheel.

In particular, eight different efficiencies have been calculated:

- η_1^{+} (from the grid to the battery): recharge efficiency, by comparing the energy output at the recharging column (i.e. measurement point M_1) and the battery energy input (i.e. measurement point M_2). This efficiency has been calculated over two complete recharges (i.e. from the minimum to the maximum allowed SOC), deriving a recharge efficiency equal to 92.0% at +25 °C and to 91.3% at −7°C.
- $\eta_2^{+/-}$ (from the battery to the EM (+) and from the EM to the battery (-)): combined efficiency of the Inverter-DC/DC, heater and EM group (dashed box in Figure 5) by comparing the mechanical energy output of the EM (i.e. measurement point M_3) with the battery energy output (i.e. measurement point M_2). This value includes the energy which flows into the low-voltages auxiliary systems and into the heating system. Plus superscript stands for driving (i.e. positive power flow, from the left to the right in Figure 5), minus superscript stands for regenerative (i.e. negative power flow, from the right to the left in Figure 5).
- $\eta_3^{+/-}$ (from the EM to the wheel (+) and from the wheel to the EM (-)): drivetrain efficiency by comparing the mechanical energy output of the EM (i.e. measurement point M_3) with the energy calculated at the wheel (i.e. measurement point M_4). As above, plus superscript stands for driving (i.e. positive power flow, from the left to the right in Figure 5), minus superscript stands for regenerative (i.e. negative power flow, from the right to the left in Figure 5).
- $\eta_{1\to3}^{+}$ (from the grid to the wheel, positive flow): by multiplying η_1^{+}, η_2^{+} and η_3^{+}.
- $\eta_{2\to3}^{+/-}$ (from the battery to the wheel and from the wheel to the battery, positive and negative flows): by multiplying η_2^{+} and η_3^{+}, and by multiplying η_2^{-} and η_3^{-} respectively.

Additionally we have estimated:

- $S_{INV-DC/DC}$: energy share which flows from the high voltage battery into the Inverter-DC/DC group.
- S_H: energy share which flows from the high voltage battery into the cabin heating system.
- E_w^{+} : driving (i.e. positive) energy at the wheel, [kWh].
- E_w^{-} : regenerative (i.e. negative) energy at the wheel, [kWh].

Please note that $S_{INV-DC/DC}$ and SH are complementary (i.e. $S_{INV-DC/DC}$ + S_H = 100%, see Figure 5), and that S_H is reported in gray for the test conditions which do not involve the use of the cabin heating system. The positive energy at the recharging station can be calculated by dividing the energy needed to drive the cycle E_w^{+} with $\eta_{1\to3}^{+}$, while the recuperated energy at the battery can be calculated

by multiplying the energy available at the wheel E_w^- with $\eta_{2\to3}^-$. The overall driving cycle efficiency $\eta_{1\to3}$ (bolded) can be calculated by equation (3):

$$\eta_{1\to3} = \frac{E_w^+}{\frac{E_w^+}{\eta_{1\to3}^+} - E_w^- \cdot \eta_{2\to3}^-} \qquad (3)$$

which is the energy needed to drive the cycle E_w^+ divided by the energy needed to drive the cycle at the recharging station minus the energy recuperated at the wheel.

The energy efficiency results, in percentage, are given in Table 7, for the same testing conditions of Table 4. The grid-to-battery η_1 efficiency is 92.0% at +25 °C and to 91.3% at −7 °C. Please note that these values have been calculated over two complete recharges, i.e. from the minimum allowed SOC of approximately 3% to the maximum allowed SOC of approximately 90%, in different climate conditions, with the same AC 3.3 kW recharging station. The battery-to-EM η_2^+ efficiency ranges from 67.3% to 91.9%, while the EM-to-battery η_2^- efficiency ranges from 23.1% to 97.3%. Both values exhibit a strong dependence on the ambient conditions and auxiliaries' load, highlighting the differences in the energy shares management (i.e. $S_{INV\text{-}DC/DC}$ and S_H) for the different conditions tested. The EM-to-wheel efficiency η_3^+ and the wheel-to-EM efficiency η_3^- exhibit instead smaller variations, i.e. from 73.7% to 86.9% and from 31.3% to 45.1% respectively. The energy efficiency cascade's steps are reported in appendix, in Figure 8, according to the schematic representation of Figure 5, for both the positive (drive) and negative (regeneration) energy flows.

The overall grid-to-wheel vehicle efficiency $\eta_{1\to3}$ results to be between 74.3% and 79.0% for the tests at +25 °C and HVAC systems switched-off, decreasing of approximately 7-to-10 percentage points by switching the HVAC system on in cooling mode. On the other hand it results between 65.9% and 71.4% at −7 °C and HVAC systems switched-off, decreasing of approximately 18-to-20 percentage points by switching the heating system on, with a higher load with respect to the cooling mode. A similar consideration can be drawn for the combined efficiencies $\eta_{1\to3}^+$ and $\eta_{2\to3}^+$, while the wheel-to-battery efficiency $\eta_{2\to3}^-$ results to be between 8.8% and 41.4%. Typically it looks to be about 30-40% for the tests with the HVAC system switched-off, to decrease to 10-20% for the tests with the HVAC system switched-on. The energy share $S_{INV\text{-}DC/DC}$ is rather high in all the testing conditions with respect to the energy share S_H, except for the −7 °C and HVAC systems switched-on tests, where we notice that the energy used for heating the cabin ranges from 21.1% to 27.1% of the energy output from the high voltage battery. This will results also in a range drop for these test conditions, as shown in the *Driving Range Results* section.

Table 7. Energy efficiency results (NEDC, WLTC and WMTC)

		NEDC [%]	WLTC [%]	WMTC [%]
$T_{Amb.}$ = +25 ºC HVAC OFF	η_1^+	92.0%	92.0%	92.0%
	η_2^+	88.8%	89.9%	91.9%
	η_2^-	82.0%	74.7%	78.5%
	η_3^+	84.6%	85.4%	86.9%
	η_3^-	45.1%	41.1%	44.3%
	$\eta_{1\to3}^+$	69.1%	70.7%	73.5%
	$\eta_{2\to3}^+$	75.1%	76.8%	79.9%
	$\eta_{2\to3}^-$	37.0%	30.8%	34.8%
	$S_{INV\text{-}DC/DC}$	99.7%	99.5%	99.8%
	S_H	0.3%	0.5%	0.2%
	E_w^+	1.39	1.39	1.39
	E_w^-	0.38	0.38	0.38
	$\eta_{1\to3}$	**74.3%**	**75.2%**	**79.0%**
$T_{Amb.}$ = +25 ºC HVAC ON	η_1^+	92.0%	92.0%	92.0%
	η_2^+	79.2%	84.5%	86.3%
	η_2^-	65.5%	57.9%	61.9%
	η_3^+	84.1%	85.0%	86.7%
	η_3^-	44.2%	40.3%	43.3%
	$\eta_{1\to3}^+$	61.3%	66.1%	68.8%
	$\eta_{2\to3}^+$	66.6%	71.9%	74.8%
	$\eta_{2\to3}^-$	28.9%	23.3%	26.8%
	$S_{INV\text{-}DC/DC}$	95.8%	96.5%	98.1%
	S_H	4.2%	3.5%	1.9%
	E_w^+	1.39	3.39	4.53
	E_w^-	0.38	0.89	1.17
	$\eta_{1\to3}$	**64.4%**	**68.9%**	**72.2%**
$T_{Amb.}$ = -7 ºC HVAC OFF	η_1^+	91.3%	91.3%	91.3%
	η_2^+	91.4%	90.7%	91.9%
	η_2^-	97.3%	84.0%	86.8%
	η_3^+	75.3%	76.0%	80.0%
	η_3^-	42.6%	31.3%	39.9%
	$\eta_{1\to3}^+$	62.9%	63.0%	67.1%
	$\eta_{2\to3}^+$	68.8%	69.0%	73.5%
	$\eta_{2\to3}^-$	41.4%	26.3%	34.7%
	$S_{INV\text{-}DC/DC}$	99.9%	99.1%	99.9%
	S_H	0.1%	0.9%	0.1%
	E_w^+	1.39	3.39	4.53
	E_w^-	0.38	0.89	1.17
	$\eta_{1\to3}$	**67.7%**	**65.9%**	**71.4%**
$T_{Amb.}$ = -7 ºC HVAC ON	η_1^+	91.3%	91.3%	91.3%
	η_2^+	67.6%	67.3%	72.8%
	η_2^-	44.0%	23.1%	34.2%
	η_3^+	73.7%	77.7%	79.6%
	η_3^-	42.1%	38.1%	39.6%
	$\eta_{1\to3}^+$	45.5%	47.8%	52.9%
	$\eta_{2\to3}^+$	49.8%	52.3%	58.0%
	$\eta_{2\to3}^-$	18.5%	8.8%	13.6%
	$S_{INV\text{-}DC/DC}$	78.0%	72.9%	78.9%
	S_H	22.0%	27.1%	21.1%
	E_w^+	1.39	3.39	4.53
	E_w^-	0.38	0.89	1.17
	$\eta_{1\to3}$	**46.6%**	**48.3%**	**53.9%**

These values are in line with those reported in literature. For example the grid-to-wheel efficiency of a BEV is suggested to be approximately 55% in 2008 [26], while 2012 studies suggest a value between 62% and 86% [16], or between 73% and 90% [27], depending on the efficiency of the vehicle's sub-systems. Moreover Tesla Motors declares to reach an overall driving efficiency of 88% [28]. A previous study from the authors suggests similar values for another tested BEV [4], as further discussed in the *Comparison of the laboratory test results with previous studies from the authors* section.

Driving Range Results

Among the topics discussed within the scientific community on the BEVs testing, the driving range test plays a fundamental role. According to the current range test [12], the type approval driving cycle has to be driven in sequence, at a temperature of +25 °C and with the auxiliary systems switched-off. The range is then determined by the cumulative distance driven up to when the vehicle is not capable to follow the duty cycle for 5 seconds, coasted-down and parked. A proposed way to estimate the driving range consists in the abbreviated test [29, 30]. One possible approach for abbreviated tests consists in applying the formula (4) considering a limited number of driving cycles:

$$Range = \frac{C}{E} D \tag{4}$$

where C is the usable battery capacity, E is the energy consumption during the test (measured at the battery level, i.e. without considering the grid-to-battery efficiency η_1) and D the distance travelled during the test. This formula allows estimating the range of the vehicle by simply scaling-up the energy demand related to a certain driving distance to the full energy capacity of the battery. The energy consumption calculation on a single driving cycle might be misleading, being the consumption for each cycle during the full-length range test different. In this work we report the driving range test results calculated with the full-length test, with one-cycle tests and with different number of cycles (i.e. multi-cycles).

Table 8. Full-length driving range test results (NEDC, WLTC and WMTC)

RANGE TEST	NEDC [km] (Wh/km – l/100km)	WLTC [km] (Wh/km – l/100km)	WMTC [km] (Wh/km – l/100km)
$T_{ambo.}$ = +25 ºC HVAC OFF	126.5 (162.0 – 1.82)	117.8 (174.1 – 1.96)	116.8 (175.6 – 1.97)
$T_{ambo.}$ = -7 ºC HVAC OFF	112.2 (182.7 – 2.05)	-	-

Table 9. Abbreviated driving range test results (one cycle)

ABBREVIATED RANGE TEST	NEDC [km]	WLTC [km]	WMTC [km]
$T_{ambo.}$ = +25 ºC HVAC OFF	130.7	114.9	112.1
$T_{Amb.}$ = +25 ºC HVAC ON	112.6	105.6	103.2
$T_{Amb.}$ = -7 ºC HVAC OFF	119.8	101.5	102.5
$T_{Amb.}$ = -7 ºC HVAC ON	82.0	73.7	76.9

In particular we have performed 4 full-length test procedures: the NEDC driving range at +25 °C and −7 °C, plus the WLTC and WMTC driving range at +25 °C. The results are reported in Table 8, including averaged energy consumption and equivalent gasoline consumption, showing a driving range from 112 to 127 km depending on the test conditions. The NEDC full-length range at −7 °C is approximately 12% shorter than the range at +25 °C, while a 7-8% range drop is found for the WLTC and WMTC range tests compared to NEDC range test.

Based on the results reported in Table 4, the one cycle abbreviated test approach has been applied by considering equation (4) in order to have an overview of the driving range depending on the different duty cycles, ambient temperatures and auxiliaries' load. The results are given in Table 9, showing a driving range between 73.7 and 130.7 km. In particular by comparing the computed range value at +25 °C and −7 °C we derive 8% to 11% range drop without HVAC and 25% to 30% range drop with the HVAC, depending on the cycle. The range values calculated with the one-cycle approach are higher than those derived with the full-length tests of approximately 3-4% at 25 °C and 7% at −7 °C.

Table 10 shows the driving range computed values by considering a variable number of cycles from the full-length range test. During the full-length tests, the vehicle was able to drive 11 NEDCs at +25 °C, 9 NEDCs at −7 °C, 5 WLTCs and 4 WMTC. The last driving cycle has been interrupted (i.e. the battery SOC did not allow to drive further). Therefore when it is used to compute the driving range with the abbreviated approach, its result is less representative that those computed on completed driving cycles, and hence it is marked in gray. Mean values and standard deviation are also reported in the summary below the table.

The results of the multi-cycles approach are reported in Table 10, for all the available cycles in each full-length range test. They show a tendency to stabilize around the full-length range test results by increasing the number of cycles considered. The driving range results reported in this section show how different test procedures and different abbreviated approaches might lead to different results. Moreover we can notice that, although the full-length driving range test can be considered the most accurate for a single specific vehicle, it might not represent the range of that vehicle's model, being a single vehicle probably affected by its driving history (e.g. aging of its battery).

Table 10. Abbreviated driving range test results (multi-cycles)

No. of Cycles [#]		NEDC (+25 ºC) [km]	NEDC (-7 ºC) [km]	WLTC (+25 ºC) [km]	WMTC (+25 ºC) [km]
1		123.6	102.6	115.4	113.2
2		124.6	106.7	116.0	113.6
3		124.0	108.1	115.7	114.1
4		124.7	109.4	116.0	118.1
5		124.6	110.0	119.1	-
6		125.0	110.5	-	-
7		125.0	110.9	-	-
8		125.3	111.1	-	-
9		125.3	112.7	-	-
10		125.4	-	-	-
11		127.2	-	-	-
Summary	mean	125.0	109.1	116.4	114.7
	std	0.917	3.004	1.518	2.276

In this work the abbreviated one-cycle and multi-cycles test procedures have been scaled on the usable battery capacity (i.e. 20.5 kWh). Nominal battery capacity might also be used, but it might lead to an overestimation of the driving range if the usable SOC is lower

than this value. Additionally, it must be highlighted that the one-cycle approach relies on the energy consumption reported in Table 4 and therefore it includes the effect of the mechanical warm-up of the car (i.e. cold-start effect).

In conclusion the one-cycle approach applied in this work, (Table 9), results to provide a slight overestimation of the driving range of the vehicle as derived by the full-length and multi-cycles range tests for the NEDC driving cycle, and a slight underestimation for the WLTC and WMTC driving cycles. However, although full-length and/or multi-cycles tests are always desirable, the one-cycle can be a useful approach to quickly estimate the range in different conditions without performing the time consuming full-length range test.

Comparison of the Laboratory Test Results with On-Road Test Results

The two parts of the present work (i.e. Part-1: Laboratory Tests and Part-2: On-road Tests) have been designed to allow a direct comparison of the results, in order to obtain a comprehensive overview of the energy consumption and driving range in type approval and real-driving test conditions for the tested BEV. This will contribute to the correlation between type approval duty cycles and real-world driving cycles as well as to the evaluation of the impact of auxiliary systems on the driving energy consumption not prescribed by the current regulation.

By comparing the distance specific energy consumption results, we derive that combined laboratory test results (at +25 °C and with the HVAC system switched-off) ranges from approximately 157 to 183 Wh/km, whereas on-road tests (performed at an ambient temperature from +21 °C to +30 °C and with the HVAC system switched-off) ranges from approximately 111 to 148 Wh/km in normal driving mode and from 109 to 139 Wh/km in economic driving mode (i.e. ECO).

By comparing the low-to-medium speed phases of the laboratory test cycles (i.e. phase 1 for the NEDC, and phases 1 and 2 for the WLTC and WMTC) with similar phases from on-road tests (i.e. phases 1 and 2 for Route 2, and phases 1, 2 and 4 for Route 3), we observe that the energy consumption from laboratory tests ranges from 144 to 174 Wh/km, whereas the energy consumption from on-road tests ranges from 85 to 161 Wh/km. Instead high-speed phases (i.e. phases 3 and 4 for WLTC, phase 3 for WMTC and phase 3 for Route 3) show energy consumption from 163 to 202 Wh/km for laboratory tests and from 155 to 158Wh/km for on-road tests.

From the results on the BEV tested we can derive that on-road tests exhibit a larger variation of energy consumption values compared to laboratory tests for low-to-medium speed phases, whereas we find the opposite trend for high-speed phases. Combined data show that laboratory test results are in line with on-road test results, with a slight tendency to provide higher consumption values (especially when compared with ECO driving mode). Therefore it is possible to conclude that the type approval test cycles are representative of the real-driving energy consumption for the tested BEV.

A similar conclusion might be drawn by looking at the one-cycle approach driving range estimate, which provides a value from 73.7 to 130.7 km for laboratory tests (at +25 °C and with the HVAC system switched-off) and from 139 to 185 km for the on-road tests (normal driving mode), showing a shorter range from the type approval tests. ECO driving mode on-road tests exhibit a range slightly higher compared to the normal driving mode, i.e. up to 188 km.

The comparison between the recuperation ratio from laboratory tests and on-road tests, at both battery and EM level, highlights higher values for on-road tests. This can be ascribed to the uncontrolled speed profile and slope variation of the on-road routes, with respect to the type approval test cycles.

Different conclusions might be derived by looking at the laboratory test results with cold ambient temperature or with the HVAC systems switched-on, as well as by looking at the on-road test results from Route 1 (uphill and downhill driving paths). Although these tests are not comparable with each other, they suggest how BEV's energy consumption might be significantly affected by ambient temperatures, auxiliaries' load and altitude's variation, elements not considered in the type approval regulation.

Comparison of the Laboratory Test Results with Previous Studies from the Authors

The laboratory test campaign presented in this paper complements and expands the pre-normative experimental activities of the Joint Research Centre. Other studies from the authors provides a better overview of the experimental activities of the group carried out on conventional fuel motorcycles and passenger cars [22, 31], HEVs and BEVs [4, 32]. In particular it might be of interest to compare the laboratory test results presented in this article with similar results from a previous campaign on a small-sized BEV, with a curb weight of 1130 kg, powered with a 47 kW electric motor and a 16 kWh Li-Ion battery. This will be later referred as E1, while the BEV tested in the present work is referred as E2. E1 was tested in 2013 in the same facility used for the present work, and only laboratory tests were carried out, therefore this comparison is not reported in the Part 2 of the work (i.e. on-road tests). The vehicle data for E1 were acquired only by CANbus (i.e. no on-board measurement clamps and ambient data sensors array).

Table 11 reports the distance specific energy consumption comparison between E_2 and E_1 in percentage, for the test conditions of Table 4. Note that E_1 was tested in the warm ambient temperature conditions at +23 °C instead of +25 °C; however this should not affect the results in a significant way. The same temperature has been instead adopted for the cold ambient temperature tests (i.e. −7 °C).

The values reported in this table show similar trends of the energy consumptions between the two laboratory test campaigns. In particular E_2 results to be more energy consuming than E_1, between 6.2% and 17.0%, at +25 °C and with both HVAC system switched-on and switched-off. Low ambient temperature causes large variations of the energy consumption, with E_2 always more energy demanding than E_1, except for the WMTC cycle at −7 °C and with the HVAC system switched-on. This is probably caused by the different working mode

of the heating system and cabin thermal inertia between the two vehicles. The recuperation ratio at the battery level also shows similar values and trend between the two vehicles, with a significant drop in both cases for the −7 °C and HVAC system switched-on test condition.

Table 11. Distance specific energy consumption comparison between E_2 and E_1 (see [4]) for the test conditions of Table 4.

Energy cons. comparison (E_2/E_1)	NEDC	WLTC	WMTC
$T_{ambo.}$ = +25 ºC/+23 ºC HVAC OFF	+18.5%	+16.3%	+9.9%
$T_{Amb.}$ = +25 ºC/+23 ºC HVAC ON	+17.0%	+13.0%	+6.2%
$T_{Amb.}$ = -7 ºC HVAC OFF	+22.0%	+15.2%	+12.3%
$T_{Amb.}$ = -7 ºC HVAC ON	-8.2%	+4.3%	-1.6%

The energy efficiency comparison between E_2 and E_1 shows a slightly higher grid-to-wheel efficiency of E_1 compared to E_2. However, no distinction between positive and negative energy flows was done for E_1, therefore a one-to-one comparison of the results is difficult.

The driving range (both from the full-length test as well as from the one-cycle abbreviated approach) is slightly higher for E_2 than for E_1, in spite of the lower efficiency, being its battery capacity higher. By comparing the grid-to-wheel energy efficiency results with the Tank-To-Wheel (TTW) efficiency reported for the hybrid vehicle (i.e. from 18 to 21%) and for three conventional fuel vehicles (from 15 to 19%) as per [4], we notice how the results from E2 confirm the findings from E_1, with a significant higher energy efficiency of the BEV with respect to conventional fuel and hybrid vehicles.

CONCLUSIONS

This paper describes the results of a test campaign carried out on a BEV, equipped with an 80 kW synchronous electric motor powered by a 24 kWh Li-Ion battery package. The test campaign includes both laboratory tests (Part-1) and on-road tests (Part-2) and this paper discuss the results from the Part-1.

As far as the laboratory tests are concerned, the vehicle has been tested over three different duty cycles (i.e. NEDC, WLTC and WMTC) at two different ambient temperatures (namely +25 °C and −7 °C), with and without the use of the cabin air-conditioning system. To further investigate this aspect, the draft MAC test procedure has been also applied. The tests have been performed in the VELA laboratories of the Joint Research Centre and the vehicle has been equipped with a programmable portable data logger capable to store and synchronize data from the vehicle's CANbus, the GPS receiver, the voltages sensors and current clamps, the thermocouples and the ambient data sensors array. A detailed description of the measurement system's specification, measurement points and experimental setup of the vehicle is also provided.

The results show that the distance-specific energy consumption of the vehicle ranges from 157 to 278 Wh/km (i.e.equivalent gasoline consumption from 1.8 to 3.1 l/100km). These tests show a grid-to-wheel efficiency of the vehicle ranging from 46.6% to 79.0%, with a marked effect of the ambient conditions and auxiliaries' load.

Four full-length driving range tests have been performed, deriving a range from 112 to 127 km, and these results have been compared with the abbreviated one-cycle or multi-cycles range calculations, providing a range between 73.7 and 130.7 km depending on the test conditions and auxiliaries' load. The results show that the results from the one-cycle and multi-cycles approaches are in line with those from the full-length tests, with only a slight overestimation of the one-cycle test for the NEDC driving cycle, and a slight underestimation for the WLTC and WMTC driving cycles.

The laboratory test results have been compared with the on-road test results, deriving that on-road tests exhibit a larger variation of energy consumption values compared to laboratory tests for low-to-medium speed phases, whereas we find the opposite trend for high-speed phases. Combined data show that laboratory test results are in line with on-road test results, with a slight tendency to provide higher consumption values, and it is possible to conclude that the type approval test cycles are representative of the real-driving energy consumption for the tested BEV.

The paper aims to provide the scientific community with experimental data to support the pre-normative research and type approval test definition for BEVs, as well as to support the calibration of BEVs' simulation models. The work aims to set the background for future technical analyses and testing activities in the fields of electric vehicles.

REFERENCES

1. Meyer, I., Wessely, S., “Fuel efficiency of the Austrian passenger vehicle fleet analysis of trends in the technological profile and related impacts on CO_2 emissions”, Energy Policy, 37 (10) (2009), pp. 3779-3789.
2. European Commission, “White Paper, Roadmap to a Single European Transportation Area - Towards a competitive and resource efficient transport system”, 2011.
3. European Commission Website, 2013. Available at: http://ec.europa.eu/clima/policies/transport/vehicles/index_en.htm. Retrieved 15-10-2014.
4. De Gennaro, M., Paffumi, E., Martini, G., Manfredi, U. et al., “Experimental Investigation of the Energy Efficiency of an Electric Vehicle in Different Driving Conditions,” SAE Technical Paper 2014-01-1817, 2014, doi:10.4271/2014-01-1817.
5. De Gennaro, M., Paffumi, E., Scholz, H., Martini, G., “GIS-driven analysis of e-mobility in urban areas: an assessment of the impact on the electric energy distribution grid”, Applied Energy, Vol. 124, 2014, pp. 94-116.
6. De Gennaro, M., Paffumi, E., Martini, G., Scholz, H., “Apilot study to address the travel behavior and the usability of electric vehicles in two Italian provinces”, Case Studies on Transport Policy, Vol. 2(3), December 2014, pp. 116-141.
7. Regulation (EC) No. 715/2007 of the European Parliament and of the Council of 20 June 2007 on type approval of motor vehicles with respect to emissions from light passenger and commercial vehicles (Euro 5 and Euro 6) and on access to vehicle repair and maintenance in formation. Eur-lex.europa.eu. Retrieved 15-10-2014.
8. Commission Regulation (EC) No. 692/2008 of 18 July2008 implementing and amending Regulation (EC) No715/2007 of the European Parliament and of the Councilon type-approval of motor

vehicles with respect to emissions from light passenger and commercial vehicles(Euro 5 and Euro 6) and on access to vehicle repair and maintenance information. Eur-lex.europa.eu. Retrieved 15-10-2014.

9. Regulation No. UN Regulation 101/2007 of the Economic Commission for Europe of the United Nations (UN/ECE) concerning the approval of passenger cars powered by an internal combustion engine only, or powered by a hybrid electric power train with regard to the measurement of the emission of carbon dioxide and fuel consumption and/or the measurement of electric energy consumption and electric range, and of categories M1 and N1 vehicles powered by an electric power train only with regard to the measurement of electric energy consumption and electric range. Eur-lex.europa.eu. Retrieved 15-10-2014.
10. Council Directive 70/220/EEC of 29 March 1970 on the measures to be taken against air pollution by emission from motor vehicles. Eur-lex.europa.eu. Retrieved 15-10-2014.
11. UNECE Website, Worldwide harmonized Light vehicles Test Procedure (WLTP), https://www2.unece.org/wiki/pages/viewpage.action?pageId=2523179. Retrieved 15-10-2014.
12. MAC test procedure to be used in a pilot phase, Final Report of the project "Collection and evaluation of data and development of test procedures in support of legislation on mobile air conditioning (MAC) efficiency and gear shift indicators (GSI)". Performed for European Commission - DG Enterprise and Industry under Framework Service Contract ENTR/05/18, 2010.
13. Paffumi, E., De Gennaro, M., Martini, G., Manfredi, U., Vianelli, S., Ortenzi, F., Genovese, A., "Experimental Test Campaign on a Battery Electric Vehicle: On-Road Test Results (Part 2)" in publication for the SAE 2015 World Congress.
14. Weiss Martin, Bonnel Pierre, Kühlwein Jörg, Provenza Alessio, Lambrecht Udo, Alessandrini Stefano, Carriero Massimo, Colombo Rinaldo, Forni Fausto, Lanappe Gaston, Le Lijour Philippe, Manfredi Urbano, Montigny Francois, Sculati Mirco, "Will Euro 6 reduce the NOx emissions of new diesel cars? e Insights from on-roadtests with Portable Emissions Measurement Systems (PEMS)", Atmospheric Environment, Vol. 62, 2012, pp. 657-665
15. Smart, J., Francfort, J., Karner, D., Kirkpatrick, M., White, S., "U.S. Department of Energy - Advanced Vehicle Testing Activity: Plug-in Hybrid Electric Vehicle Testing and Demonstration Activities", 24th Electric Vehicle Symposium Proceedings (EVS 24), 2009.
16. Faria, R., Moura, P., Delgado, J., de Almeida, A. T., "A sustainability assessment of electric vehicles as a personal mobility system", Energy Conversion and Management Journal, Vol.61, 2012.
17. Alessandrini, A., Orecchini, F., Ortenzi, F., Campbell, F.V., "Drive-style emissions testing on the latest two Honda hybrid technologies", European Transport Research Review, Volume 1, Issue 2, pp. 57-66, July 2009.
18. Alessandrini, A., Cattivera, A., Filippi, F., Ortenzi, F., "Driving style influence on car CO2 emissions", 20th International Emission Inventory Conference, 2012.
19. GPSvisualizer Home Page, http://www.gpsvisualizer.com/, Retrieved 15-10-2014.
20. National Instruments website, www.ni.com. Retrieved 15-10-2014.
21. Eurins website, www.eurins.com. Retrieved 15-10-2014.
22. IEC 61851-1: Electric vehicle conductive charging system-Part 1: General requirement.
23. SAE International Surface Vehicle Standard, "Shear Adhesion Test for Glass Bonding Adhesive Systems," SAE Standard J1722. work in progress
24. Martini, G., Manfredi, U., and De Gennaro, M., "Gaseous Emissions from Euro 3 Motorcycles and Euro 5 Passenger Cars Measured Over Different Driving Cycles," SAE Technical Paper 2013-01-2619, 2013, doi:10.4271/2013-01-2619.
25. Environmental Protection Agency (EPA), EV Label, http://www.epa.gov/otaq/carlabel/electriclabelreadmore.htm#2. Retrieved 15-10-2014.
26. European Green Vehicles Initiative, "European Roadmap Electrification of Road Transport, Version 2.0", November 2010, http://www.egvi.eu/, Retrieved 15-10-2014.
27. Helmers, E., Marx, P., "Electric cars: technical characteristics and environmental impacts", Environmental Sciences Europe, 2012.
28. Tesla Motors Website, http://www.teslamotors.com/goelectric/efficiency, Retrieved 15-10-2014.
29. Meyer N., Whittal I., Christenson M., Loiselle-lapointe A., "The impact of the driving cycle and climate on electrical consumption and range of fully electric passengers vehicles", Proceedings of EVS 26, 2012.
30. SAE International Surface Vehicle Recommended Practice, "Battery Electric Vehicle Energy Consumption and Range Test Procedure", SAE Standard J1634, Rev. Oct. 2012.
31. De Gennaro, M., Paffumi, E., Martini, G., Manfredi, U., Rossi, R., Massari, P., Roasio, R., "Gaseous Emissions from Gasoline-to-CNG/LPG Converted Motorcycles", in publication for the SAE 2015 World Congress.
32. Simic, D., Dvorak, D., Lacher, H., Kuehnelt, H. et al., "Modeling and Validation of Lithium-Ion Battery based on Electric Vehicle Measurement," SAE Technical Paper 2014-01-1850, 2014, doi:10.4271/2014-01-1850.

ACKNOWLEDGMENTS

The authors would like to acknowledge the essential contribution of the JRC VELA laboratory staff. A special acknowledgement goes to Prof. Valerio Fiorentino Conte and Mr. Jim Pollock for their support.

DEFINITIONS/ABBREVIATIONS

AC - Alternating Current

BEV - Battery EV

CJT - Cold Junction Compensation

CPU - Central Processing Unit

DC - Direct Current

DoH - Degree of Hybridization

ECO - ECOnomic driving mode

EM - Electric Motor

FPGA - Field Programmable Gate Array

GHG - Greenhouse Gas

LDV - Light Duty Vehicle

HEV - Hybrid EV

MAC - Mobile Air-Conditioning

NEDC - New European Driving Cycle

NMEA - National Marine Electronics Association

PEMS - Portable Emissions Measurement System

SOC - State of Charge

TTW - Tank-To-Wheel

UNECE - United Nation Economic Commission for Europe

UTM - Universal Transverse Mercator

WLTC - World-wide harmonized Light vehicles Test Cycle

WMTC - World-wide Motorcycle emission Test Cycle

APPENDIX

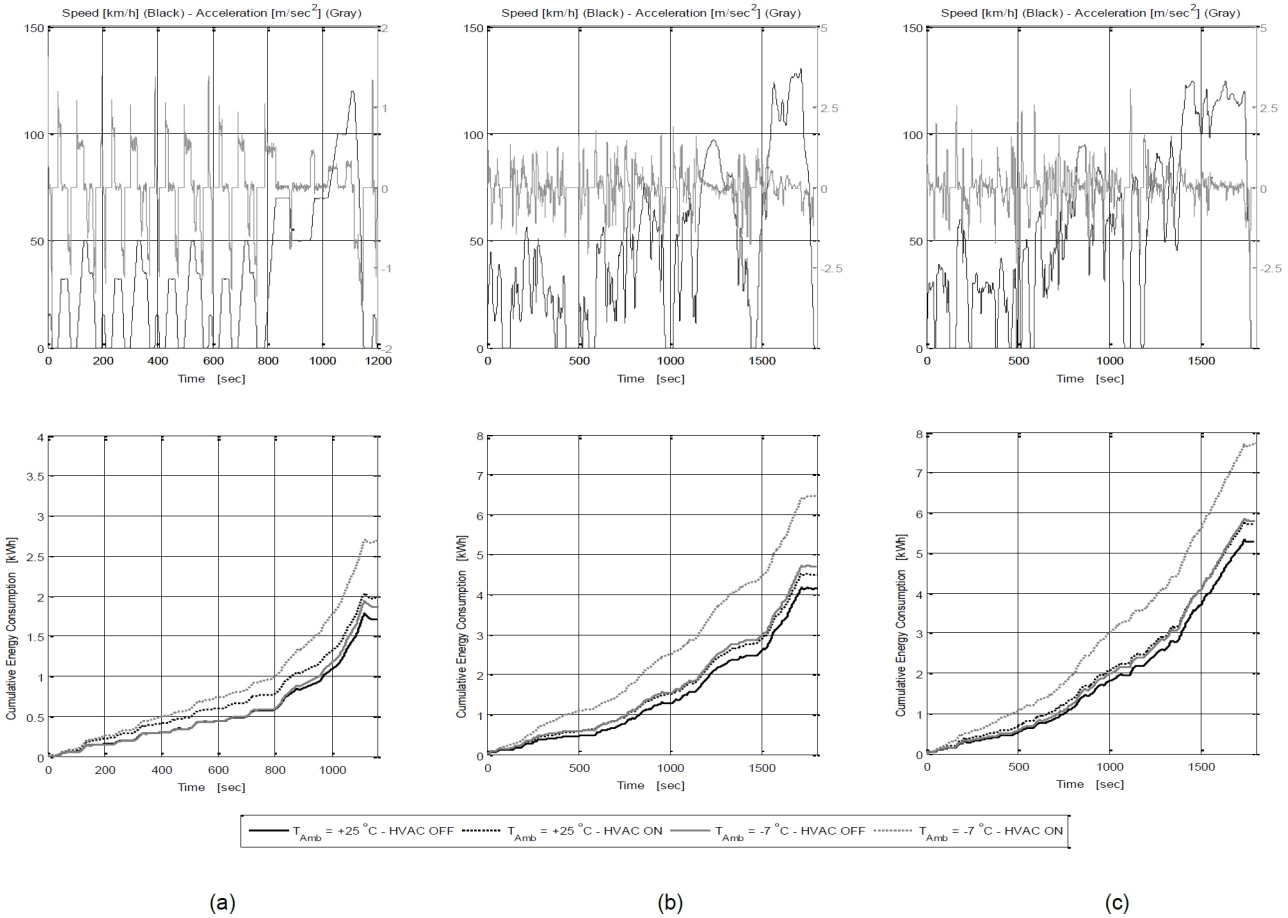

Figure 6. Speed profile, acceleration profile and second-by-second cumulative energy consumption in [kWh] over the NEDC (a), WLTC (b) and WMTC (c) driving cycles for the four testing conditions considered (+25 °C/−7 °C, HVAC on/off).

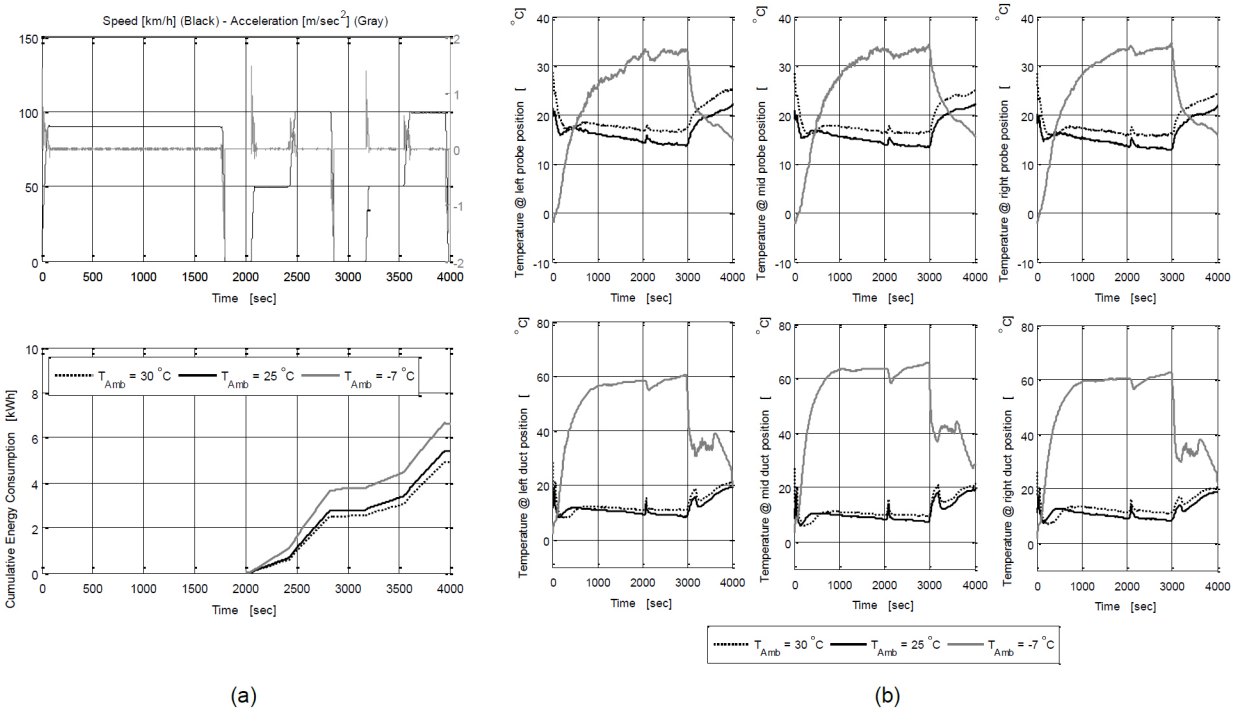

Figure 7. Speed profile, acceleration profile and second-by-second cumulative energy consumption in [kWh] over the MAC driving cycle (a) and thermocouples measurements (b). Left, mid and right probe positions correspond to driver's head, between the driver's and the passenger's seat and behind the passenger's head, whereas left, mid and right duct positions correspond to the left, mid and right outlet of the HVAC system located on the dashboard. Mid duct temperature is the average between the mid-left and mid-right duct measurements.

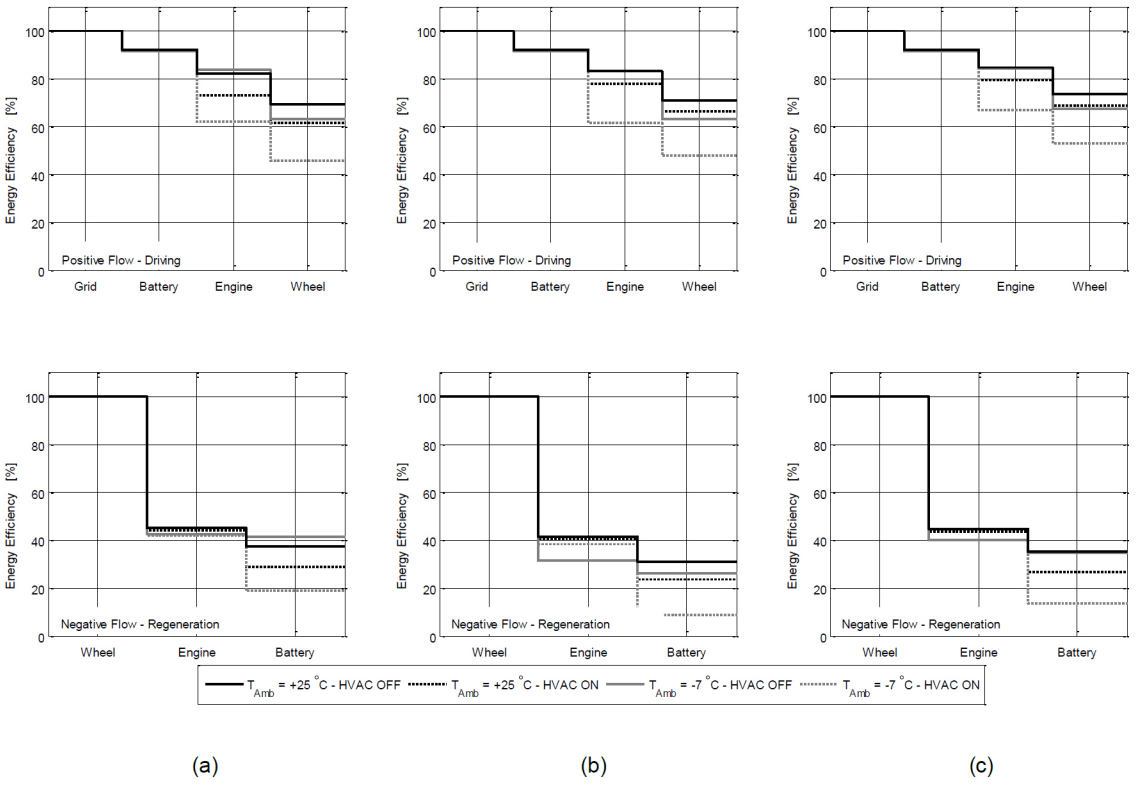

Figure 8. Efficiency cascade results for positive (drive) and negative (regeneration) power flow for the NEDC (a), WLTC (b) and WMTC (c) driving cycles, for the four testing conditions considered (+25 °C/−7 °C, HVAC on/off). The cascade's steps are reported according to Figure 5.